Shallow landsliding, root reinforcement, and the spatial distribution of trees in the Oregon Coast Range

Joshua J. Roering, Kevin M. Schmidt, Jonathan D. Stock, William E. Dietrich, and David R. Montgomery

Abstract: The influence of root reinforcement on shallow landsliding has been well established through mechanistic and empirical studies, yet few studies have examined how local vegetative patterns influence slope stability. Because root networks spread outward from trees, the species, size, and spacing of trees should influence the spatial distribution of root strength. We documented the distribution and characteristics of trees adjacent to 32 shallow landslides that occurred during 1996 in the Oregon Coast Range. Although broadly classified as a conifer-dominated forest, we observed sparse coniferous and abundant hardwood trees near landslide scars in an industrial forest (Mapleton) that experienced widespread burning in the 19th century. In industrial forests that were burned, selectively harvested, and not replanted (Elliott State Forest), swordfern was ubiquitous near landslides, and we observed similar numbers of live conifer and hardwood trees proximal to landslide scarps. We demonstrate that root strength quantified in landslide scarps and soil pits correlates with a geometry-based index of root network contribution derived from mapping the size, species, condition, and spacing of local trees, indicating that root strength can be predicted by mapping the distribution and characteristics of trees on potentially unstable slopes. In our study sites, landslides tend to occur in areas of reduced root strength, suggesting that to make site-specific predictions of landslide occurrence slope stability analyses must account for the diversity and distribution of vegetation in potentially unstable terrain.

Key words: slope stability, vegetation, root strength, shallow landslide, debris flow, Oregon Coast Range.

Résumé : L'influence de l'armature des racines sur les glissements superficiels a été bien établie par des études mécaniques et empiriques; par contre, peu d'études ont examiné comment les réseaux végétatifs locaux influencent la stabilité des talus. Parce que les réseaux de racines s'étalent à partir des arbres, les espèces, la dimension et l'espacement des arbres devraient influencer la distribution spatiale de la résistance des racines. On a documenté la distribution et les caractéristiques des arbres adjacents à 32 glissements superficiels qui se sont produits en 1996 dans la chaîne de montagnes de la côte de l'Oregon. Quoique classifiée généralement comme une forêt dominée par les conifères, on a observé des conifères clairsemés et des arbres de bois francs en abondance près des cicatrices de glissements dans une forêt industrielle (Mapleton) qui a été affectée par des incendies très étendues au 19^{e} siècle. Dans les forêts industrielles qui ont été brûlées, exploitées de façon sélective, et non reboisées (Elliot State Forest), les fugères étaient omniprésentes près des glissements et on a observé un nombre identique de conifères et de bois francs vivants à proximité des cicatrices de glissement. On démontre que la résistance des racines quantifiée dans les cicatrices de glissement et dans des excavations est en corrélation avec un indice de contribution du réseau de racine basé sur la géométrie dérivée de la cartographie de la dimension, des espèces, de la condition et de l'espacement des arbres sur des talus potentiellement instables. Sur nos sites d'étude, les glissements ont tendance à se produire dans les zones où la résistance des racines est réduite, ce qui suggère que pour faire des prédictions d'occurrence de glissement sur un site donné, les analyses de stabilité de talus doivent tenir compte de la diversité et de la distribution de la végétation sur un terrain potentiellement instable.

Mots clés : stabilité de talus, végétation, résistance des racines, glissement superficiel, écoulement de débris, chaîne de montagnes de la côte de l'Oregon.

[Traduit par la Rédaction]

Received 19 June 2001. Accepted 1 November 2002. Published on the NRC Research Press Web site at http://cgj.nrc.ca on 27 February 2003.

J.J. Roering.[1] Department of Geological Sciences, University of Oregon, Eugene, OR 97403–1272, U.S.A.
K.M. Schmidt. United States Geological Survey, 345 Middlefield Rd, MS 975, Menlo Park, CA 94025, U.S.A.
J.D. Stock and W.E. Dietrick. Department of Earth and Planetary Science, University of California, Berkeley, Berkeley, CA 94720–4767, U.S.A.
D.R. Montgomery. Department of Earth and Space Science, University of Washington, Seattle, WA 98195–1310, U.S.A.

[1]Corresponding author (e-mail: jroering@oregon.uoregon.edu).

 doi: 10.1139/T02-113

Introduction

Shallow landsliding is a primary erosional process in many soil-mantled, mountainous landscapes. Typically comprised of colluvial sediments, shallow slope failures often initiate in unchanneled valleys or steep slopes, mobilize into debris flows, and travel long distances through the low-order channel network, scouring and depositing sediment along their paths (e.g., Swanston and Swanson 1976; Dietrich and Dunne 1978; Okunishi and Iida 1981; Johnson and Rodine 1984; Fannin and Rollerson 1993; Benda and Dunne 1997). In addition to degrading aquatic habitat and water quality, shallow landslides and debris flows can endanger infrastructure and human life (Fannin et al. 1997; Rollerson et al. 1997). Extreme rainfall events generate shallow slope failures by elevating pore pressures and decreasing effective stress, but numerous site-specific factors, such as preferential hydrologic flowpaths, slope steepness, soil thickness, and material properties influence the potential for slope instability (e.g., Wilson and Dietrich 1987; Buchanan and Savigny 1990; Johnson and Sitar 1990; Iverson and Reid 1992; Reid and Iverson 1992; Iverson et al. 1997; Montgomery et al. 1997; Bovis and Jakob 1999). Field observations and experimental data attest to the importance of tree roots for providing shear strength to shallow forest soils (e.g., Burroughs and Thomas 1977; Waldron 1977; Abe and Ziemer 1991; Kuruppuarachchi and Wyrwoll 1992; Riestenberg 1994; Wu 1995; Gray and Sotir 1996; Watson et al. 1999), although few studies have addressed how temporal and spatial variations in forest characteristics may affect root strength and shallow landsliding.

Tree roots have the ability to resist tension, thereby increasing the shear strength of shallow soils through mechanical reinforcement (e.g., O'Loughlin 1974; Shewbridge and Sitar 1989; Skaugset 1997). In forested mountainous regions, such as the Oregon Coast Range (OCR), landslide scarps often reveal broken root tendrils, suggesting that the tensile strength of the roots was mobilized during failure (Schmidt et al. 2001). Numerous researchers have quantified how root reinforcement influences the shear strength of soil (e.g., Burroughs and Thomas 1977; Ziemer 1981; Riestenberg and Sovonick-Dunford 1983; Shewbridge and Sitar 1989; Sidle 1992; Gray and Sotir 1996; Schmidt et al. 2001).

By studying how the tensile strength of roots is mobilized during shear failure, Waldron (1977) and Wu et al. (1979) established a methodology for converting the tensile strength associated with individual root tendrils to an equivalent cohesion (often termed the "apparent cohesion due to root reinforcement"). Other studies employed this technique to explore the variability of root strength associated with tree species and age (Burroughs and Thomas 1977; Waldron and Dakessian 1981; Wu 1995; Schmidt et al. 2001). Riestenberg (1994) extended the methodology to account for the spatial distribution of root networks, calculating the critical density of sugar maple trees necessary to stabilize soils. Thus far, these studies have focused on the root strength associated with individual trees and their root networks. It has not been shown that their findings can be extended to estimate how root strength varies spatially and temporally across forested landscapes.

Numerous studies have attempted to explore linkages among root strength, landsliding, and forest management through analyses of landslide density in forests of varying stand age and land-use history (Brown and Krygier 1971; Ketcheson and Froehlich 1978; Swanson et al. 1981; Amaranthus et al. 1985; Montgomery et al. 2000). Several of these studies indicate that the density of landslides in areas that have recently been clearcut exceeds the landslide density observed in natural forests by at least 2–3 times and in some cases by more than an order of magnitude (Swanson et al. 1981; Ziemer 1981; May 1998; Montgomery et al. 2000; Snyder 2000). These studies do not directly address the mechanisms by which root reinforcement affects shallow landsliding because they do not incorporate information about roots or vegetation present in the immediate vicinity of landslide scars. Forested landscapes are often characterized and classified by the stand age of the dominant trees despite the variability of canopy size and structure (Swanston et al. 1988; Robison et al. 1999). Sidle and Wu (Sidle 1992; Wu and Sidle 1995; Sidle and Wu 1999) have evaluated the potential for shallow landsliding on a regional basis by assigning spatially uniform values of root cohesion according to forest stand age.

Spatial variability of forest characteristics, however, can be substantial. The species, density, age, and condition of trees reflects the legacy of land use, fire, erosion, and disease in a particular landscape. The density, tensile strength, and depth of roots vary significantly with species. Furthermore, cycles of tree senescence will affect the frequency and magnitude of root strength in areas prone to shallow landsliding. Few studies have systematically explored the influence of local vegetation on landslide occurrence. A framework for linking the characteristics and distribution of trees with quantitative estimates of root strength will improve our ability to identify potentially unstable areas and evaluate the implications of land management practices.

This contribution introduces a new dataset describing "above ground" vegetation patterns adjacent to landslide sites and relates it to root strength variability in landslide scarps and soil pits reported by Schmidt et al. (2001). Here, we investigate the influence of local vegetation on root strength and shallow landsliding by (1) documenting the species, size, and condition of trees surrounding 32 shallow landslide scarps in two Oregon study sites to (*a*) determine whether landslides tend to exploit gaps in the coniferous canopy, and (*b*) quantify vegetation variations in mature coniferous forests; and (2) developing a quantitative methodology for estimating root strength using maps of the characteristics and distribution of local trees on a potentially unstable hillslope. Because landslides are a highly localized phenomenon that reflect site-specific conditions, our results highlight the important influence of local vegetation patterns on the potential for slope instability.

Slope stability model for shallow forest soils

The Coulomb–Terzaghi failure criterion predicts slope instability when shear stress (kPa), τ, equals or exceeds shear strength because of cohesion and frictional resistance

$$[1] \qquad \tau \geq C_s + C_r + \sigma' \tan\phi$$

where C_s and C_r (kPa) are cohesion because of soil and root strength, respectively, σ' is effective normal stress (kPa), and ϕ is the internal angle of friction (°). Upon invoking the assumptions of an infinite slope (Lambe and Whitman 1969), eq. [1] can be used to assess the stability of shallow soil-mantled hillslopes where $\tau = \rho_s g z \sin\theta\cos\theta$ and $\sigma' = (\rho_s - \rho_w M) g z \cos^2\theta$; ρ_s and ρ_w are the density of soil and water ($kg \cdot m^{-3}$), respectively, g is acceleration due to gravity ($m \cdot s^{-2}$), z is soil depth (m), M is the ratio of the height of the piezometric surface above the base of the soil (h) to the total vertical soil thickness (z), and θ is the slope angle (°). This implementation assumes slope-parallel groundwater flow; Reid and Iverson (1992) discuss the influence of alternative flow regimes on slope stability.

In humid forests, soil moisture is relatively high and it is common for root networks to grow laterally or parallel to the slope. In unchanneled valleys, soils are typically thick enough (>1 m) that tree roots often do not penetrate the bedrock surface (e.g., in the Pacific Northwest Coast Ranges, Dietrich and Dunne 1978). Trees common to humid, mountainous landscapes (such as Western hemlock (*Tsuga heterophylla*), cedar (*Thuja plicata*), and Douglas-fir (*Pseudotsuga menziesii*)) grow tap roots. However, in relatively shallow coarse-grained soils, these tap roots are typically diverted parallel to the slope (Eis 1974, 1987).

Equation [1] can be adapted to incorporate lateral root reinforcement on forested hillslopes (Riestenberg and Sovonick-Dunford 1983; Wu 1984; Burroughs 1985; Reneau and Dietrich 1987; Terwilliger and Waldron 1991; Montgomery et al. 2000), such that stress and strength components are partitioned along the basal and lateral surfaces of a potentially unstable soil mass

$$[2] \qquad A_b \rho_s g z \sin\theta\cos\theta \geq A_b(C_{sb} + C_{rb}) + A_L(C_{sL} + C_{rL}) + A_b[(\rho_s - \rho_w M) g z \cos^2\theta \tan\phi]$$

where A_b and A_L are area of the basal and lateral boundaries, respectively, C_{sb} and C_{rb} are cohesion along the basal surface owing to soil and root reinforcement, respectively, and C_{sL} and C_{rL} are cohesion along the lateral margins owing to soil and root strength, respectively (Cuthbertson 1992). Although Burroughs (1985) and Cuthbertson (1992) included terms to represent shear strength due to buttressing and arching contributions, we neglect those terms in this contribution because of the lack of compelling evidence in the field and the difficulty of recreating tree configurations prior to failure. This formulation (eq. [2]) simplifies the mechanical complexities introduced by upslope and downslope stresses acting on the slide mass and thus should be used for comparative estimates of how root reinforcement influences slope stability.

Equation [2] allows root cohesion to be estimated by back-calculation, given estimates of C_s and ϕ and an assumption about the position of the water table. Most back-analysis studies assume that the water table is at the land surface ($M = 1$) and root cohesion acts only along the base of the slide mass (i.e., $C_{rL} = 0$, Wu et al. 1979). Estimates of root strength, C_r, associated with coniferous trees (Burroughs and Thomas 1977; Schmidt et al. 2001) are high enough that eq. [2] does not predict instability for saturated slopes ($M = 1$) with values of C_s, ϕ, z, and θ typical of many forested landscapes (Yee and Harr 1977; Wu et al. 1979; Schroeder and Alto 1983; Burroughs 1985). As a result, landslides in forested terrain may be strongly influenced by diverse vegetation patterns and patches of low root strength.

Root networks

In humid, coniferous forests, the lateral extent of tree root networks increases with tree diameter and mirrors the crown coverage (Ross 1932; McMinn 1963; Kochenderfer 1973; Eis 1974, 1987; Coutts 1983). The magnitude of root strength in a potentially unstable soil mass will increase with the amount and extent of adjacent root networks. In other words, the distribution of trees surrounding a potential landslide site controls the apparent cohesion owing to root strength (Riestenberg 1994).

In natural forests that have been undisturbed for several hundred years by timber harvesting or fire, a recent study reveals extremely high values of root cohesion (Schmidt et al. 2001), exceeding 50 kPa in some areas. Such high values reflect the dominance of several large-diameter roots, as the branching behavior of root networks can be complex. Although many factors may influence the morphology of root networks (including slope angle, soil and bedrock types, soil moisture, species, hillslope aspect, and interaction with other trees) the lateral extent of root systems can be predicted from observations of tree species and stem diameter (Smith 1964).

Tree species has an important influence on the temporal and spatial distribution of root strength. Whereas the tensile load at failure associated with individual root tendrils of a given diameter does not vary significantly among different tree species found in the OCR (Schmidt et al. 2001), the depth, density, and size distribution of roots depends strongly on species. In addition, the life span of different species varies according to environmental factors as well as natural limits to tree maturation. Disturbances in forests, such as landslides and fires, alter the local environment, producing a complex mosaic of vegetation. Our analysis focuses on using tree distributions and root network geometry to quantify lateral root strength in the OCR.

To explore whether landslides in forested terrain tend to occur in areas with a dearth of significant coniferous tree cover (and thus root strength), we mapped trees around shallow landslide scarps and estimated root cohesion by inventorying exposed broken roots.

Study sites: Oregon Coast Range

In February 1996, high-intensity storms triggered thousands of shallow landslides in the OCR. The 4-day rainfall total exceeded 700 mm in many areas and the maximum daily total was 208 mm (Taylor 1997). In November 1996, another intense storm produced over 220 mm of rainfall over a 3-day period, triggering widespread slope failures and causing six fatalities. Landslides occurred in state, federal, and private lands and in areas under various states of management. The Oregon Department of Forestry (ODF) conducted a storm impact study in several regions of the OCR to document the character and frequency of landslides in

forests with different management histories. Their results suggest that in recently (<10 years) clearcut terrain the frequency of landslides because of the 1996 storms exceeds that in 100+ year-old stands (Robison et al. 1999). In addition, they report similar landslide densities in 100+ year-old stands and areas that had been clearcut 10–30 years prior to the 1996 storms. This surprising observation motivated efforts to clarify mechanical controls on landsliding in +100-year stands.

In steep, soil-mantled landscapes, such as the OCR, shallow landslides are a primary mechanism by which sediment is transported from hillslopes to channel networks (Dietrich and Dunne 1978). Soil-mantled hillslopes in parts of the OCR are steep (sometimes exceeding 40°) and typically exhibit alternating sequences of ridges and unchanneled valleys. Soils on ridges generally do not exceed 1 m in depth, whereas in unchanneled valleys, soil depths vary from 1 to 3 m (Dietrich and Dunne 1978; Montgomery et al. 1997; Schmidt 1999). In unchanneled valleys (or hollows), sediment accumulates over 100- to 1000-year timescales and soil age may vary with position along the hollow axis (Reneau 1988; Benda 1990; Reneau and Dietrich 1990). On hourly timescales, rainfall events cause sub-surface storm flow to concentrate in hollows (Montgomery et al. 1997), generating elevated pore pressures that can destabilize the soil and lead to debris flow mobilization (Pierson 1977; Iverson 2000). These debris flows travel several metres per second, usually through the established valley network, and vary in volume from several hundred to several thousand cubic metres.

We visited three forested areas with similar underlying bedrock (greywacke, Tyee Formation) in the central OCR that experienced widespread shallow landsliding because of the 1996 storms (Fig. 1). In the ODF Mapleton study area, the February 1996 storms generated thousands of shallow landslides in recently clearcut and forested terrain. The forested terrain has been undisturbed since the 1860s when large fires swept through the area and burned substantial portions of the central OCR (United States Geological Survey 1898). We observed an abandoned logging road along one of the major ridges in the 100+ year-old stand portion of the Mapleton study site, although it is not proximal to landslide sites and thus did not likely influence the hydrologic response. In the Elliott State Forest (ESF) study area, the November 1996 storms generated hundreds of landslides in terrain of varied management history (Fig. 2). Whereas one section of the ESF study area exhibits 300+ year-old Douglas-fir trees (Silver Creek stand), most of the surrounding forested terrain was burned over 150 years ago and selectively logged in the 1960s (the lasting influence of these practices on root strength is discussed in Schmidt et al. (2001)). Finally, we quantified the distribution of trees and root strength in two unfailed, unchanneled valleys in the Hubbard Creek basin with 200+ year-old Douglas-fir trees.

Tree mapping and root strength characterization

Methods

To explore how local tree cover may influence root strength and slope stability, we documented the distribution of trees around 32 landslide scarps in the Mapleton and ESF

Fig. 1. Location figure of OCR showing the location of our three study areas: Mapleton, ESF (which includes Silver Creek stand), and Hubbard Creek. We analyzed: 21 landslides in Mapleton, 11 landslides and 2 soil pits in ESF, and 2 soil pits in Hubbard Creek. For further data on the Mapleton and ESF sites, see Robison et al. (1999).

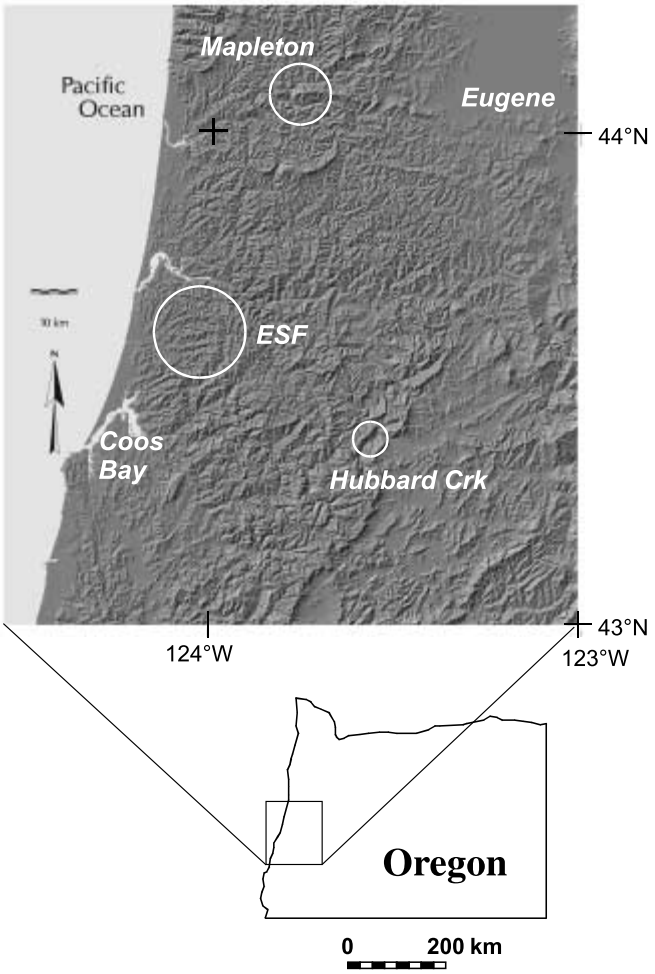

study areas. We visited landslides in the summer of 1997, focusing on shallow landslides that mobilized into debris flows, as these events had the largest impact on the downstream channel network. Most of the landslides we visited had been identified and mapped by Robison et al. (1999), whose protocol entailed walking all channels in the study areas to look for landslides because landslide density can be underestimated when measured solely by the use of air photos. At each site, we quantified landslide scarp morphology (including length, width, depth of soil (measured vertically), and slope of the initial failure site) and mapped all trees within 14 m of the landslide scarp (including species, diameter at breast height (dbh), condition (live, dead, or cut), and distance to scarp (measured horizontally)) (Fig. 3). Here, we define the landslide scarp as the headscarp and lateral margins of the failure initiation site. We measured tree-to-scarp distances to within 0.1 m and soil and rooting depths to within 0.05 m. For our calculations, we distinguished among hardwood trees, including red alder (*Alnus rubra*), bigleaf maple (*Acer macrophyllum*), vine maple (*Acer circinatum*),

Fig. 2. Photograph of a landslide scar in the ESF study site that occurred during the November 1996 storms. Notice the predominance of swordfern surrounding the scar and the lack of proximal coniferous vegetation. A dead conifer stem (snag) stands upslope of the scarp and live Douglas-fir trees are predominant further upslope. A live hemlock tree can be seen in the right side of the photograph. The base of this tree is downslope of the scarp and lies more than 10 m from the edge of the scarp. The width of the scar is approximately 5 m.

cascara (*Rhamnus purshiana*), beaked hazelnut (*Corylus cornuta*), and red elder (*Sambucus racemosa*), and coniferous trees, including Douglas-fir (*Pseudotsuga menziesii*) and western hemlock (*Tsuga heterophylla*).

In addition to characterizing the surrounding vegetation, we quantified root strength for 12 of the landslide scarps (in the Mapleton and ESF study areas) and for four soil pits (in the Silver Creek stand (within ESF) and Hubbard Creek study area) with a root inventorying procedure (Schmidt et al. 2001). Estimates of tensile strength can be converted to apparent root cohesion (quantified with units of stress) by dividing the tensile force due to root strength by the lateral surface area of the soil column across which the roots act (Wu 1995). We estimated values of tensile strength (quantified as load at failure) due to root strength by measuring the diameter, species, condition, depth, and orientation of all

Fig. 3. Schematic depicting tree mapping adjacent to a landslide scarp. The species, dbh, condition (live, dead, cut) and tree-to-scarp distance were documented for all trees within 14 m of landslide scarps.

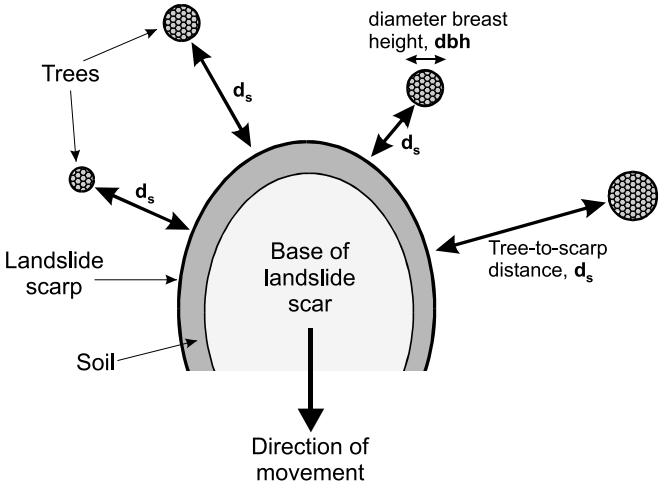

broken roots greater than or equal to 1 mm in diameter within landslide headscarps and lateral margins. In the four soil pit sites, we measured roots that intersected the margins of the excavations.

Results

Distribution of trees near shallow landslides

Our tree mapping results illustrate how vegetative patterns vary within forested landscapes. Aerial photographs suggest that both the Mapleton and ESF study areas are characterized by dense, coniferous stands. Indeed, through the course of our fieldwork, we observed a predominance of Douglas-fir and western hemlock species. However, the character of vegetation proximal to landslide scarps varied significantly, both within and between the two study areas.

In the Mapleton study area, we observed dense understory vegetation beneath Douglas-fir and hemlock trees of varying age (some more than 100-years-old). The vegetation was dominated by mature red alder, vine maple, and big leaf maple trees. Adjacent to 21 landslide scarps, we mapped the local tree distribution and grouped the trees into five categories: live coniferous, dead coniferous, cut coniferous, live hardwood, and dead hardwood. Histograms of tree-to-scarp distance for these five tree categories show a preponderance of live hardwood trees surrounding the headscarps (Fig. 4). Over 125 live hardwood trees were observed within 10 m of the 21 landslide scarps. Red alder trees accounted for the majority of these hardwoods and were typically found just upslope of the landslide headscarps. In addition, we observed a scarcity of live coniferous trees near landslide scarps in the Mapleton study area; fewer than 10 were observed within 8 m of all 21 scarps. Furthermore, at least 10 dead coniferous trees (2–10 m high snags in various states of decay) were observed within 10 m of the headscarps. Thus, vegetation in the immediate vicinity of shallow landslide initiation sites does not reflect the broad classification as a dense, coniferous forest.

Fig. 4. Histogram describing the tree-to-scarp distance, d_s, for all trees within 14 m of 21 landslides in the Mapleton study area. See text for species included in hardwood and conifer categories. Note the preponderance of hardwood trees near landslide scarps and the paucity of live coniferous trees.

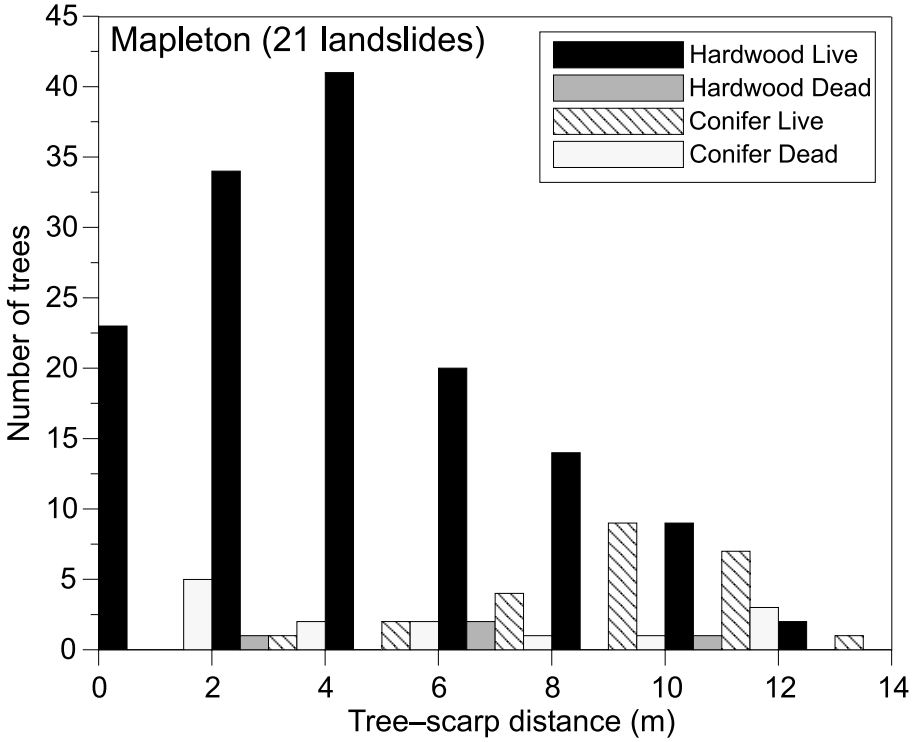

In the ESF study area, the understory vegetation was sparse and consisted primarily of swordfern (*Polystichum munitum*). Douglas-fir and western hemlock trees dominated the canopy. For the 11 shallow landslide sites we visited, we observed roughly equal numbers of live hardwood and coniferous trees within 8 m of the headscarps (Fig. 5). The average number of live trees within 14 m of the landslides was less than that observed in the Mapleton study area. Nonetheless, more coniferous trees were observed around landslide scars in the ESF study area and hardwood trees were less common than in the Mapleton area. We observed at least 10 conifer stumps and 7 dead conifers around the headscarps. The roots associated with these dead or cut trees were brittle upon handling (thus providing negligible strength) and many roots associated with live conifers exhibited signs of disease and poor health (Schmidt et al. 2001).

To further characterize the vegetative pattern around each landslide, we calculated the mean tree-to-scarp distance for the five tree categories at each of the 32 landslides in the Mapleton and ESF study areas. Figure 6 illustrates the normalized distribution of mean tree-to-scarp distance for each landslide and shows that the average distance to coniferous trees is greater than that for hardwood trees. The fractional value denotes the percentage of landslides with a particular tree-to-scarp distance for a given tree category. For over 60% of the landslides, the average distance to a live hardwood tree is less than 6 m, whereas almost 80% of the landslides had an average distance to live coniferous trees of greater than 6 m. Dead coniferous, dead hardwood, and cut coniferous trees were distributed at various distances from landslide headscarps, suggesting that landslides may occur in areas with decreased root strength.

Tree and root characteristics

Figures 7 and 8 illustrate the distribution of dbh for trees in our study sites. These measurements reflect the size and development of the trees and can be used to extrapolate properties of their associated root networks. In both of our study sites, live coniferous trees exhibited large dbh values, with over 50% having dbh greater than 0.7 m. In contrast, live hardwood trees had the smallest dbh values, as 50% had a dbh of less than 0.2 m. As documented in the forestry literature (e.g., Worthington et al. 1962; Trappe et al. 1968), hardwoods and in particular red alder, have a competitive advantage over coniferous trees in recently disturbed terrain and in frequently saturated soils because of their ability to fix nitrogen. The preponderance of hardwood trees near many of the landslide scarps may attest to the history and distribution of disturbance because of land-use practices and erosional processes. In addition, hardwood trees, such as red alder, often have a limited life span (typically <70 years, Trappe et al. 1968), such that periods of decreased root reinforcement may be more frequent in hardwood-dominated forest patches.

The distributions of live coniferous and hardwood rooting depths are illustrated using box plots in Fig. 9. Both distributions decline exponentially with depth and have similar median values (30 and 35 cm for the hardwood and coniferous roots, respectively). However, the live conifer category has significantly more deep roots, as over 25% of the roots were observed to be deeper than 60 cm. In addition, 10% of the live coniferous roots were found at depths greater than 90 cm, compared to less than 0.5% for the hardwood roots. The depth of rooting controls the volume of soil that may be reinforced with roots and thus the size of potential

Fig. 5. Histogram describing the tree-to-scarp distance, d_s, for all trees within 14 m of 11 landslides in the ESF study area. See text for species included in hardwood and conifer categories. Note the approximately equal numbers of live hardwood and coniferous trees adjacent to landslide scarps.

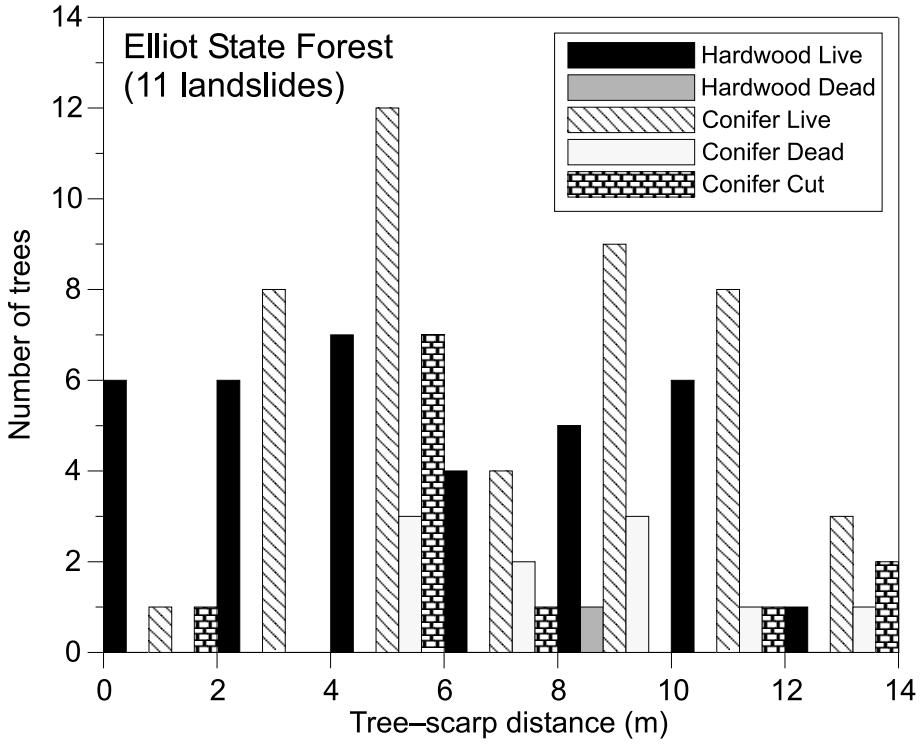

Fig. 6. Histogram illustrating the fraction of landslides with a given mean tree-to-scarp distance for various tree categories (32 total landslides in the Mapleton and ESF study sites). At over 55% of the landslide sites, the mean distance from the scarp to a live coniferous tree exceeds 8 m. See text for description.

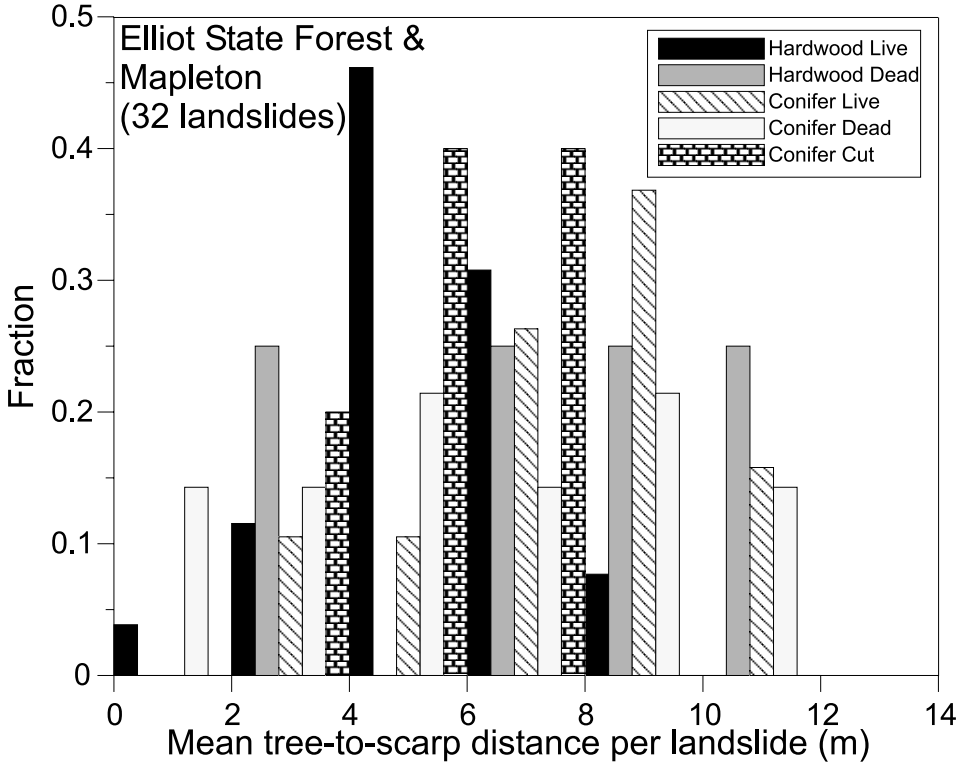

Fig. 7. Box plot depicting the observed distribution (dots) and quantiles of dbh (m), for various tree categories in the Mapleton study area. Dead and live conifers exhibited the largest dbh values, whereas live hardwood trees had consistently low dbh values. The line inside the box signifies the median dbh and the top and bottom of the box delineate the 75th and 25th percentile values, respectively. The high and low horizontal bars denote the dbh associated with the 90th and 10th percentile values, respectively.

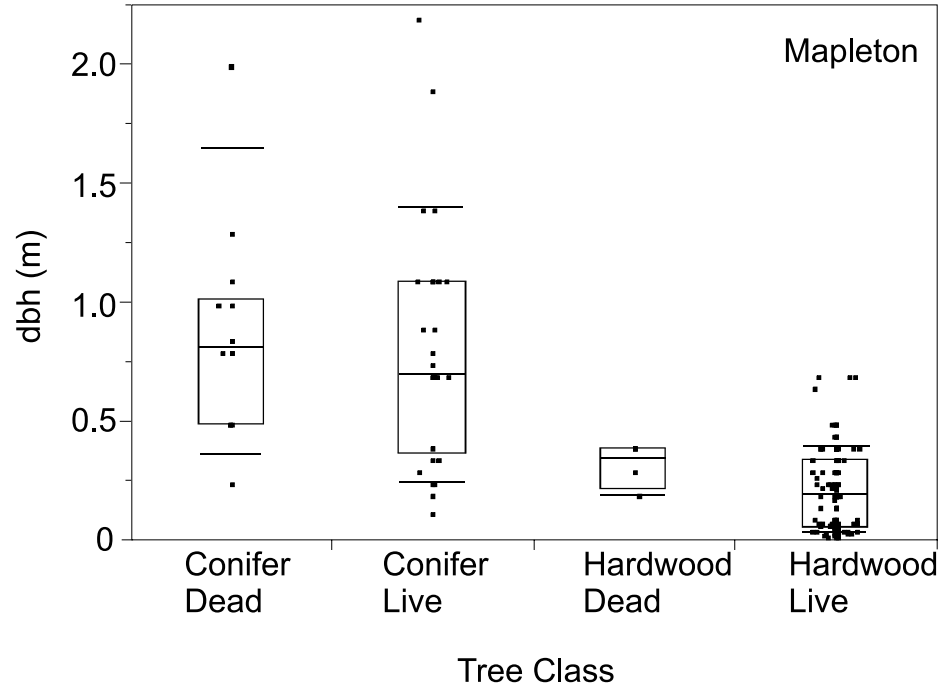

Fig. 8. Box plot depicting the observed distribution of dbh (m) for various tree categories in the ESF study area. See Fig. 7 caption for description of box plot designations.

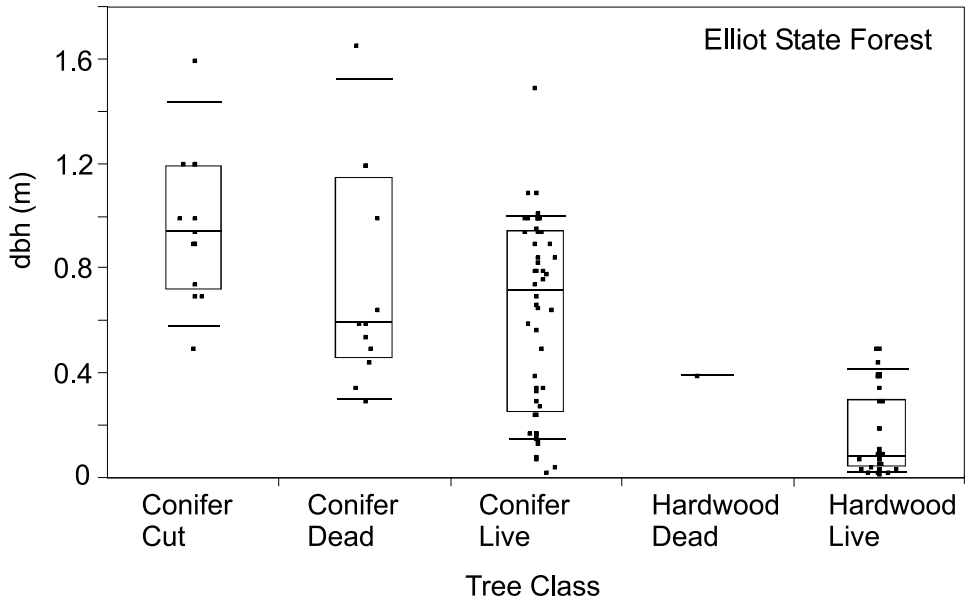

landslides. As described by Schmidt et al. (2001), the average depth of the landslides we observed is approximately 1.0 m. As Fig. 9 demonstrates, hardwood trees contributed root reinforcement only to the shallow sections of the landslide masses, whereas the coniferous roots penetrated deeper, providing more extensive root reinforcement. In addition, previous studies indicate that coniferous root networks tend to be denser than hardwood networks (Wu 1995).

Correlation of root strength with the spatial distribution of trees

To relate the spatial distribution of live trees to root strength in the underlying soil, we devised a simple geomet-

Fig. 9. Box plot describing the rooting depth distribution for live conifer and hardwood roots in our three study areas (Mapleton, ESF, and Hubbard Creek). Box plot designations are the same as those described in Figs. 7 and 8. Both distributions are approximately exponential, although the conifer roots were consistently deeper than the hardwood roots.

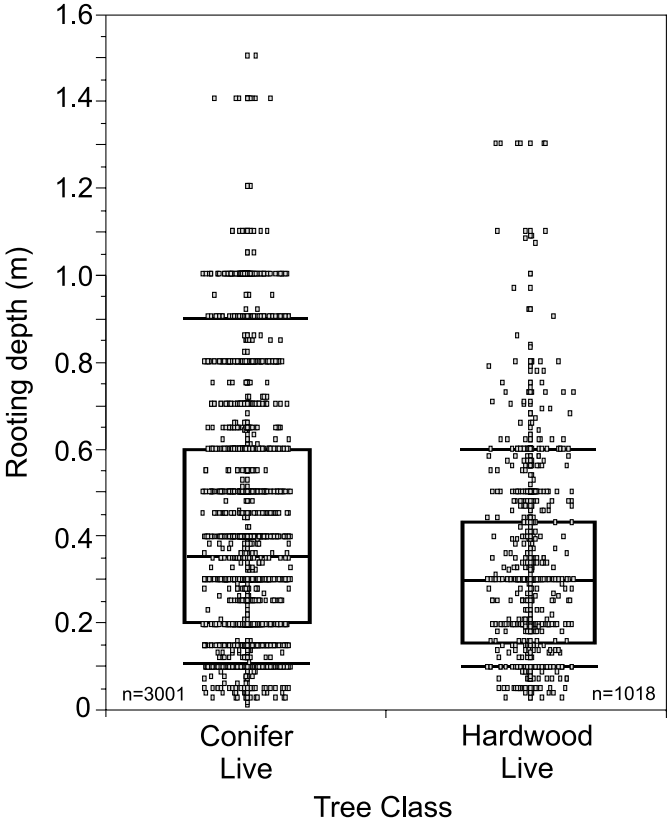

Fig. 10. Log-log plot illustrating the relationship between dbh (m) and crown and root network radius (m) of Douglas-fir trees. Crown and root network radii are well-correlated (McMinn 1963; Smith 1964), such that crown radius can be used to approximate root network radius. Crown radius points were obtained from Maguire (personal communication, 2000) and from our field measurements. Root network radius values were given by McMinn (1963). Root network and crown radius varies as a power function of dbh (eq. [3]).

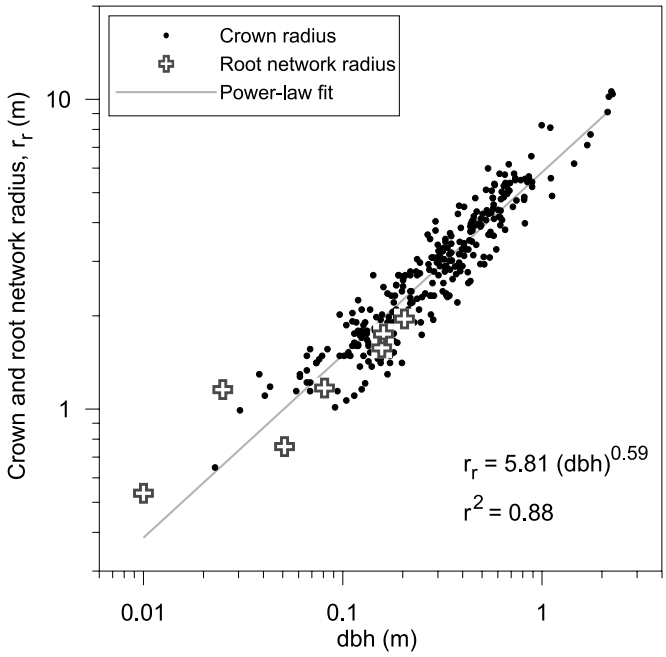

ric technique using our tree mapping results and root strength estimates obtained by Schmidt et al. (2001). Roots add shear strength to soil when the root network penetrates a potential failure surface. The amount of tensile root force contributed to a potential slide mass should increase with increasing area of root intersection. Hence, we explored how the tensile strength estimated by the root inventory method varies with the cross-sectional area of root network intersection with landslide scarps. We analyzed how the distribution of all live trees may contribute to root reinforcement and performed a separate analysis for live coniferous trees because they are more likely to provide long-term root strength to the soil column. We only characterized root strength along the upslope headscarp and lateral margins of landslides, as roots along the downslope margin are incorporated into the landslide mass and their contribution to shear strength cannot be easily quantified.

Quantification of root network characteristics in areas prone to shallow landsliding is critical for linking local vegetation patterns and root reinforcement. Despite numerous complexities that influence the development of trees and root networks (Stone and Kalisz 1991), the spatial extent of root networks increases systematically with the trunk diameter of trees. Furthermore, the radius of Douglas-fir and hemlock root networks is well-correlated with tree crown radius (McMinn 1963; Smith 1964). To quantify the root network area (in planview) for individual trees, we utilized correlations of dbh and tree crown – root network radius reported for coniferous trees (primarily Douglas-fir, McMinn 1963; Smith 1964; Eis 1974; Maguire and Hann 1989; D. Maguire, personal communication, 2000) (Fig. 10). These data suggest that the root network radius (defined as the spatial extent of roots ≥1 mm), r_r, increases with dbh according to a power-law relationship:

$$[3] \qquad r_r = A(dbh)^B$$

where A is 5.8 ± 0.9, B is 0.59 ± 0.01 and r_r and dbh are given in metres (r^2 = 0.88). For our analyses of hardwood tree root networks, we also used eq. [3] because the relevant data are lacking.

To quantify the intersection of root networks with landslide scarps we used a simple geometric technique, approximating landslide scars and soil pits as circular arcs (Fig. 11). We determined the effective radius of scarp and pit boundaries by measuring the basal area of the scarp or soil pit and calculating an equivalent radius (see Table 1). Although most scarps are somewhat elongated along the downslope axis, sensitivity analyses suggest that our circular approximation doesn't significantly influence the following analyses. The vertical cross-sectional area along a scarp intersected by a root network (termed root–scarp area (RSA) and defined as the product of the length along the scarp (root–scarp length, RSL) and the average vertical soil depth

along the scarp), may act as a surrogate for root strength and can be calculated according to

$$[4] \quad \mathrm{RSA} = d_L \mathrm{RSL} = d_L 2r_s \cos^{-1}\left(\frac{r_s^2 + (d_s + r_s)^2 - r_r^2}{2r_s(d_s + r_s)}\right) \quad \text{where } r_r > d_s$$

$$\mathrm{RSA} = 0 \qquad \text{where } r_r \le d_s$$

where d_L is average soil depth along the landslide scarp over which roots may be present (m), r_s is scarp radius (m), d_s is tree-to-scarp distance (m), and r_r is root network radius (m) (Fig. 11). The $\cos^{-1}$ term is calculated in radians. At each site, we calculated RSA for all live trees ($\mathrm{RSA_{all}}$) and live coniferous trees ($\mathrm{RSA_{con}}$), respectively. We did not include dead or cut trees, because tensile strength decreases exponentially with time following tree expiration and becomes negligible compared with the live tensile strength (Burroughs and Thomas 1977; Schmidt et al. 2001). In addition, we selected 1.0 m as the maximum allowable value of d_L, as 95% of the conifer roots we observed were shallower than 1.0 m (Fig. 9). For each landslide and soil pit, we calculated RSA for each surrounding tree and summed the non-zero RSA values of all live trees (coniferous and hardwood), $\Sigma\mathrm{RSA_{all}}$, and live coniferous trees, $\Sigma\mathrm{RSA_{con}}$, separately.

Schmidt et al. (2001) estimated the tensile force at failure due to all live and live coniferous tree roots, T_{all} and T_{con} ($\mathrm{kg \cdot m \cdot s^{-2}}$), respectively, in 12 landslide and 4 soil pit locations where we mapped the nearby distribution of trees. To relate the local pattern of tree cover to subsurface root tensile force, we plotted $\Sigma\mathrm{RSA_{all}}$ and $\Sigma\mathrm{RSA_{con}}$ against T_{all} and T_{con}, respectively, for the 12 landslides and 4 soil pits and observed a positive correlation for both datasets (Figs. 12A and 12B). We observed a weakly defined linear relationship for both cases ($T_{all} = 12.0\ \Sigma\mathrm{RSA_{all}} + 63.4$, $r^2 = 0.55$ and $T_{con} = 11.9\ \Sigma\mathrm{RSA_{con}} + 41.5$, $r^2 = 0.61$). The data suggest increasing root reinforcement with proximity and extent of nearby root systems. Nine of the 16 sites exhibited $\Sigma\mathrm{RSA_{con}}$ values equal to 0, as sparse coniferous trees were found nearby. For these sites, Schmidt et al. (2001) estimated low values of tensile strength owing to coniferous roots, consistent with our proposed linkage between tree spacing and root strength. For both fits (Figs. 12A and 12B), the regression intercept was positive, indicating that small but finite values of tensile force were observed when ΣRSA equals zero. This suggests that root networks may be slightly more extensive than predicted by our power-law dbh relationship (eq. [3]). Deviations from the observed linear relationship may also reflect variability in root network properties as well as measurement uncertainties. For example, at site silcrk1 (a soil pit site that did not experience root breakage by mass movement), approximately 44% of the root strength owing to live coniferous roots results from two roots with diameter greater than 50 mm ($\Delta T_{>50mm}$ in Figs. 12A and 12B denotes the amount of tensile force associated with these two large roots), as this site exhibits anomalously high tensile force relative to $\Sigma\mathrm{RSA_{all}}$ and $\Sigma\mathrm{RSA_{con}}$.

To account for the dominant influence of large-diameter roots on root reinforcement in our study sites, we reanalyzed the relationship between root tensile strength and root network – scarp intersection, including only roots with diameter less than 10 mm (Figs. 12C and 12D). By considering only abundant, smaller-diameter roots (<10 mm) in our calculation of T_{all} and T_{con}, we may obtain an estimate of the minimum amount of root strength and avoid the tendency for sporadic large-diameter roots to impart dominance on strength measurements. Furthermore, the inclusion of large-diameter roots may overestimate strength because the tensile strength of large roots may exceed the pull-out resistance (force required to overcome soil–root bonds and extrude roots from the soil column), such that the tensile strength of large roots may not be fully mobilized during shear failure (Waldron and Dakessian 1981). As depicted in Figs. 12C and 12D, for a given value of $\Sigma\mathrm{RSA_{con}}$ or $\Sigma\mathrm{RSA_{all}}$, the magnitude of root strength (T_{con} or T_{all}) is smaller than that predicted when all roots are considered. For both datasets (all trees and coniferous trees), we observe an improved linear relationship with ($T_{all} = 6.29\ \Sigma\mathrm{RSA_{all}} + 22.8$, $r^2 = 0.74$ and $T_{con} = 6.47\ \Sigma\mathrm{RSA_{con}} + 13.4$, $r^2 = 0.80$). These relationships for roots with diameter <10 mm may represent the minimum amount of root strength provided by adjacent trees. Large roots may provide further reinforcement by resisting soil displacement and sharing the imposed load during shearing of the soil column, although the kinematics and timing of loading is difficult to quantify (Stolzy and Barley 1968; Waldron 1977; Shewbridge and Sitar 1989).

Fig. 11. Schematic illustrating a geometric technique for estimating the magnitude of root strength provided by trees adjacent to landslides. The RSL (m) is the along scarp distance over which a root network intersects the landscape scarp (as approximated by a circular arc). For this example, $\Sigma\mathrm{RSL} = \mathrm{RSL_1} + \mathrm{RSL_2}$. The ΣRSA ($\mathrm{m^2}$) is quantified by multiplying ΣRSL by the average soil depth along the landslide scarp, d_L (here, the maximum value is limited by the depth of rooting ~1 m). The root network radius, r_r, is estimated using field measurements of dbh and eq. [3]. Effective scarp radius, r_s, and tree-to-scarp distances, d_s, are measured in the field. For each landslide or soil pit, we calculated the sum of non-zero values of RSA.

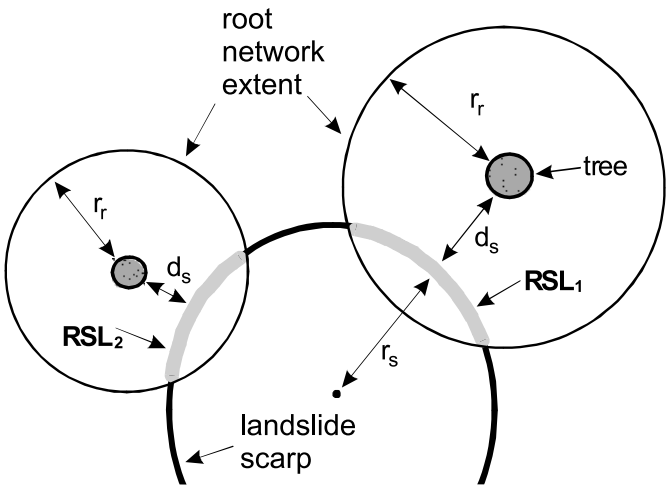

Discussion

Spatial variation in canopy structure

Our analyses indicate that the spacing, size, and condition of trees control the spatial pattern of root strength and

Table 1. Summary of landslide and soil pit root strength and tree spacing data.

Site	Scarp length (m)	Scarp width (m)	Scarp basal area (m^2)	Effective basal radius*, r_s (m)	Slope (°)	ΣRSL_{all} (m)	ΣRSL_{con} (m)	Average soil depth, d_L (m)	ΣRSA_{all} (m^2)	ΣRSA_{con} (m^2)	T_{all} ($kg \cdot m \cdot s^{-2}$)	T_{con} ($kg \cdot m \cdot s^{-2}$)	T_{all} ($kg \cdot m \cdot s^{-2}$) roots <10 mm	T_{con} ($kg \cdot m \cdot s^{-2}$) roots <10 mm
Map307	8.2	7.6	62.3	4.45	43	7.04	0	0.72	5.07	0	139	2.89	59.7	1.24
Map328	8.6	6.8	58.5	4.31	38	13.2	0	0.83	10.9	0	322	35.9	117	13
Esf1	16	11.2	179	7.55	42	0	0	0.51	0	0	99.5	32.6	65.1	21.3
Esf2	9.14	7.9	72.2	4.79	44	9.24	0	1.07	9.24	0	81.8	5.16	52.9	3.34
Esf3	5.5	5.74	31.5	3.17	46	0	0	0.74	0	0	47.8	44.9	42.9	40.4
Esf4	3.5	2.1	7.35	1.53	44	0	0	0.17	0	0	2.9	2.9	0	0
Esf5	4.8	3	14.4	2.14	47	0	0	0.48	0	0	4.51	4.25	3.49	3.29
Esf6	6.9	4.93	34	3.29	40	22.3	22.3	1.64	22.3	22.3	322	320	207	206
Esf7	6.6	6.8	44.9	3.78	43	18.5	18.5	1.19	18.5	18.5	220	183	95.9	79.9
Esf9	5.2	2.2	11.4	1.91	45	3.87	3.27	1.02	3.87	3.2	77.0	61.7	37.9	30.4
Esf10	1.7	3.3	5.61	1.34	34	0	0	0.62	0	0	28.5	23.2	20.9	17
Esf11	8.8	4.57	40.2	3.58	32	1.99	1.99	1.09	1.99	1.99	47.4	44.1	33.9	31.6
Esf11a (p)	1.5	1	1.5	0.69	32	4.64	4.64	1.3	4.64	4.64	76.4	75.7	34.2	33.8
Silcrk1 (p)	1.5	1	1.5	0.69	34	5.34	5.34	1.25	5.34	5.34	319	317	44.3	44.1
LitshaA (p)	1.5	1	1.5	0.69	34	6.1	6.1	0.94	5.73	5.73	179	155	51.4	44.6
LitshaB (p)	1.5	1	1.5	0.69	34	0	0	1.46	0	0	106	91.6	49.4	42.8

Note: Map, denotes Mapleton study area (industrial forest, widespread burning in the 19th century); Esf, denotes Elliott State Forest (industrial forest, clearcut 1890s without replanting, commerical thinning in the 1960s); Silcrk, denotes Silver Creek stand within Elliott State Forest (natural forest with 300-year-old trees); Litsha, denotes Hubbard Creek study area (natural forest with 200-year-old trees); ΣRSA_{all} and ΣRSA_{con} are calculated as the product of d_L and ΣRSL_{all} and ΣRSL_{con}, respectively (see eq. [4]), where the maximum value of d_L is 1.0 m, as limited by the depth of rooting; and (p) designates soil pit sites.
*The effective scarp basal radius is calculated according to: $r_s = \sqrt{(\text{length} \times \text{width})/\pi}$.

Fig. 12. Plots of total root tensile strength (T_{all} and T_{con}) as a function of our geometric root network factor (ΣRSA) for (A) all live trees, (B) live conifer trees, (C) all live trees and roots <10 mm in diameter, and (D) live conifer trees and roots <10 mm in diameter. The sites are described in Table 1 (see Schmidt et al. (2001) for details on tensile strength calculation). A positive correlation is observed for all four datasets. The thin black lines are linear regression fits and the associated equations are shown on the graph. At some sites (particularly silcrk1), a significant fraction of the root strength results from a limited number of large-diameter roots. The thick gray vertical arrows in (A) and (B) labeled with $\Delta T_{>50mm}$ denote the amount of root strength attributed to two conifer roots with diameter >50 mm at the silcrk1 site.

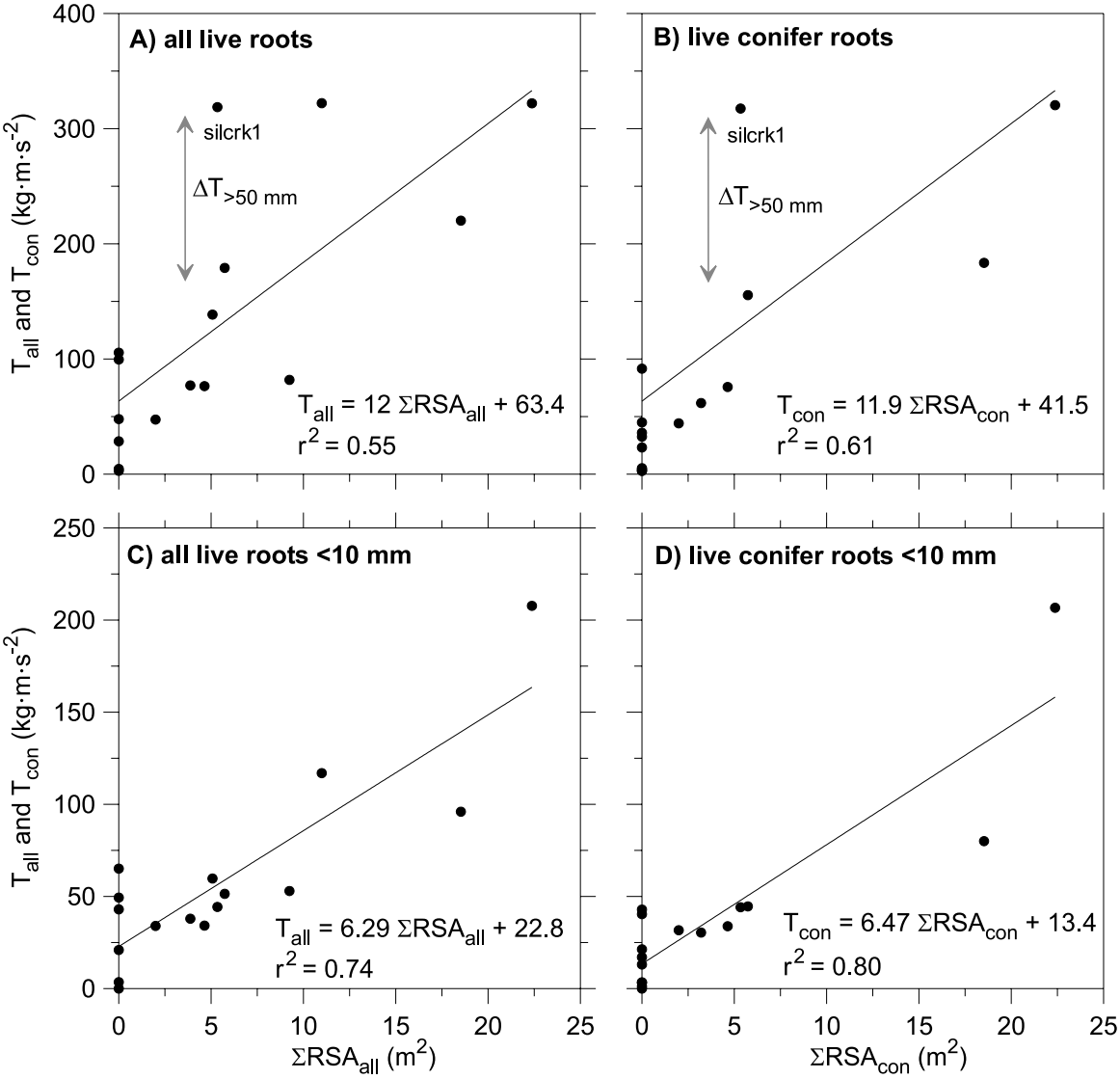

influence the location of shallow landsliding in forests. The mosaic of vegetation in forests reflects the history of land-use practices (including timber harvesting and burning), climate, and erosional processes. Importantly, the variable character of trees near landslide sites in our study sites implies that broad species and (or) timber age classifications may not be appropriate for assessing how local vegetation influences slope stability. In the Mapleton study area (characterized as a predominantly coniferous forest), short-lived, shallow rooting hardwood species dominated the local vegetation near most of the landslides we visited, suggesting that biological and hydrological processes may affect how the distribution of coniferous trees evolves in areas prone to shallow landsliding (Shainsky et al. 1992; Bailey et al. 1998; Wardman and Schmidt 1998; Van Pelt and Franklin 1999). Aerial photographs of the low-order channel network reveal the dominance of hardwood species in the Mapleton study area, suggesting that these areas may be prone to frequent disturbance or hydrologic conditions that do not favor conifers. However, the relative importance of altered hydrologic conditions and disturbance legacy on hardwood growth is difficult to decipher. Although the Mapleton study area has not been actively managed for timber production in the last 100 years, it experienced widespread burning in the past several hundred years. In the context of slope stability, the importance of such activities remains poorly quantified. We do not suggest that an abundance of hardwood trees on potentially unstable hillslopes is a necessary condition for shallow landsliding. Instead, we propose that landslides may exploit gaps in the coniferous canopy. The predominance of

hardwood trees in certain areas of the Mapleton study site may reflect the legacy of large fires and (or) timber harvests, which may affect landscapes, and particularly landslide-prone areas, for hundreds of years or more. Most generally, our results demonstrate the importance of documenting the local vegetation when assessing local slope stability.

Our results only address the current vegetation conditions adjacent to landslide sites, although the dynamics of forest stand succession will certainly impart a crucial control on slope stability. In addition, the spatial variability of tree and understory vegetation in our study sites suggests that regional slope stability analyses could be significantly augmented with detailed characterizations of local vegetation patterns. In contrast to the assignment of landscape-wide root strength values (Dietrich et al. 1995; Sidle and Wu 1999), more detailed descriptions of canopy structure (Spies and Franklin 1991) may help to account for spatial variations in root strength.

Conceptual methodology for estimating root cohesion from tree mapping

The positive correlation between tensile strength estimates and the distribution of adjacent trees may be used to evaluate the magnitude of reinforcement in potentially unstable areas. The data necessary to estimate root strength can be readily collected in the field. We propose the following conceptual methodology to estimate tensile strength because of roots: (1) identify potentially unstable terrain (topographic-based slope stability analyses may provide a regional assessment (Montgomery and Dietrich 1994; Wu and Sidle 1995; Montgomery et al. 2000)), (2) within a potentially unstable area (e.g., steep, unchanneled valley), map the local distribution of trees (including species, dbh, and condition) and measure slope angle and average vertical soil depth, (3) calculate the root network radius, r_r, for all live and coniferous trees using eq. [3] (or an alternate dataset appropriate for the relevant tree species), and plot the location of tree trunks and root networks in planview as to best visualize their distribution across the hillslope, (4) choose a representative landslide scarp radius (this can be estimated from regionally-based empirical datasets or theoretical analyses), and find the scarp location that minimizes ΣRSL; although elegant and thorough search algorithms may be employed to find the minimum value of ΣRSL, a simple iterative procedure of graphically moving the scarp amongst the root networks and recalculating ΣRSL should yield an accurate estimate, (5) multiply the minimum value of ΣRSL by the average soil depth to obtain ΣRSA, and use the linear regression coefficients shown in Fig. 12 to calculate the magnitude of tensile strength because of root reinforcement, and (6) convert the estimate of tensile strength to a cohesion value by dividing by the perimeter area along the potential landslide lateral margin and multiplying by an empirical constant, 1.2 (see Schmidt et al. 2001). Estimates of root cohesion can then be included in slope stability analyses that account for lateral strength (e.g., eq. [2]). In landscapes where significant root reinforcement acts through the basal boundary of shallow landslides, additional data relating the depth and distribution of basal roots should be incorporated to account for basal anchoring of roots.

Example calculation: Mapleton study site

To illustrate how the technique may be applied, we mapped a potential debris flow source area in our Mapleton study site that did not fail in the 1996 storms. The topographic hollow had similar characteristics to landslide sites in the Mapleton and ESF study areas (Fig. 13). The data necessary to construct the tree map and estimate root cohesion were collected using a series of simple and straightforward measurements requiring a tape measure, hand level (or inclinometer), and soil auger. Figure 13 depicts the hollow geometry and the distribution of coniferous trees and their associated root networks (root network radii were calculated with eq. [3]). Average soil depth (d_L) is 1.1 m and the slope along the hollow axis is approximately 40°. All of the root networks shown emanate from live Douglas-fir trees. To be consistent with characteristic shallow landslides observed during the 1996 storms in the OCR (Robison et al. 1999), we chose a representative landslide scarp radius (r_s) of 3 m. By iteratively moving the circular scarp along the hollow axis and recalculating ΣRSL, we position the scarp as to minimize ΣRSL (in this case, the minimum value is ΣRSL = RSL_1 + RSL_2 = 11.6 m and the total angle along the circular scarp intersected by root networks is 3.9 radians or 222°). The ΣRSA is calculated as the product of d_L (the maximum value is 1.0 m as limited by the rooting depth) and ΣRSL (giving ΣRSA = 11.6 m^2). The linear regression coefficients in Fig. 12 are used to calculate the associated tensile strength for two cases: (1) live conifer roots (T_{con} = 179 $kg \cdot m \cdot s^{-2}$, see Fig. 12B) and (2) live conifer roots <10 mm in diameter (T_{con} = 88.5 $kg \cdot m \cdot s^{-2}$, see Fig. 12D). We converted these two estimates of root strength to lateral root cohesion values by dividing by the lateral perimeter area of the scarp ($A_L = 1.5\pi r_s d_L$ = 14.1 m^2) and multiplying by an empirical coefficient, 1.2, (see eq. [5], Schmidt et al. 2001). Although the total circumference of the idealized circular base equals $2\pi r_s$, we seek to estimate the distance along the headscarp and lateral margins (~75% of the total circumference) because the downslope portion of the scarp is incorporated into the landslide mass. From this procedure, we estimate 15.2 and 7.5 kPa of lateral root cohesion, for the analyses with conifer roots and conifer roots <10 mm, respectively.

Equation [2] predicts that under conditions of saturated slope-parallel flow (M = 1), our study hillslope requires 11 kPa of lateral root cohesion (C_{rL}) to maintain stability (given estimates of the angle of internal friction (40°), basal scarp area ($A_b \approx \pi r_s^2$ = 28 m^2), ρ_s = 1.7 $g \cdot cm^{-3}$, ρ_w = 1.0 $g \cdot cm^{-3}$, and negligible soil cohesion ($C_{sL} = C_{sb} = 0$)), whereas for half-saturated conditions (M = 0.5) 5.5 kPa of cohesion is required. The root cohesion estimate derived from our tree mapping procedure and the amount required for stability are of similar magnitude, suggesting that this unchanneled valley may be vulnerable to shallow landsliding during intense rainfall events. Significant uncertainties remain regarding the relative importance of pore pressure generation as hydrologic response can be difficult to constrain. Although this calculation incorporates numerous simplifications and approximations, it may capture the general tendency of root networks to spread outward from trees and reinforce nearby soils. We intend that this approach be useful for comparative estimates of site-specific root strength

Fig. 13. Planview map of an unchanneled valley in the Mapleton study area that did not fail during the 1996 storms. The distribution of trees and root networks (calculated with eq. [3]) most relevant to slope stability are plotted. Gray lines are topographic contours that depict a topographic hollow in the center that drains downward. Douglas-fir tree trunks and their associated root networks are indicated by fill-shaded gray circles and black circles, respectively. Through an iterative search, the location of a landslide scarp (with an effective radius of 3 m) that minimizes ΣRSL is shown by the hachured circular arc, wherein the total arc length of the scarp intersected by root networks ($\Sigma RSL = RSL_1 + RSL_2$) is 11.6 m. See text for description of how this value is converted to root cohesion and incorporated into a slope stability analysis.

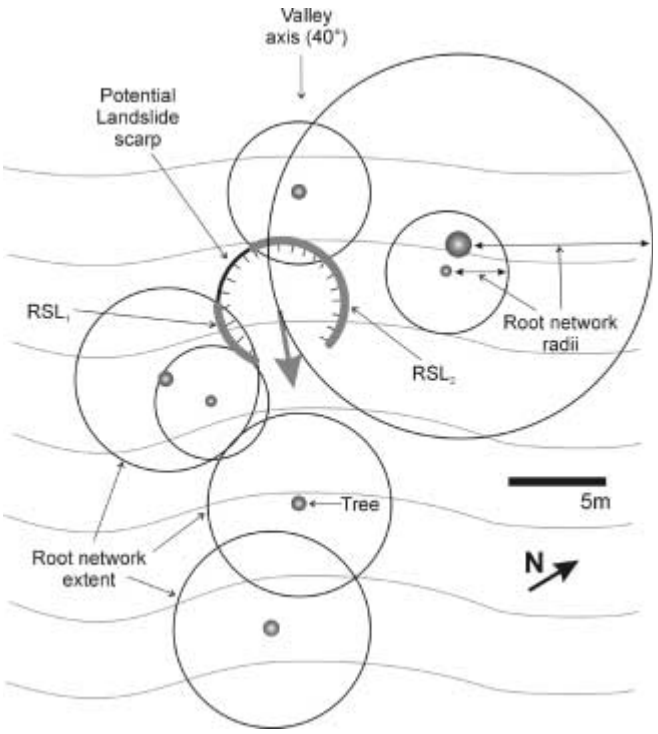

and the calculated values should be viewed as such upon consideration of the assumptions invoked. The step of arbitrarily designating a landslide scarp size (r_s) requires further justification, possibly through detailed analysis of empirical data and mechanistic models for landslide development (Okimura 1983).

Tree spacing and slope stability

Previous studies have used the characteristics of root systems and slope stability analyses to estimate the spacing of trees necessary to decrease the likelihood of shallow landsliding (Riestenberg 1994; Krogstad 1995; Wu 1995). These studies assume uniform spacing of trees, typically achieved through replanting. Importantly, these studies recognize the variability of root networks and the influence of root diameter on lateral root strength. In contrast, our simple model allows for the estimation of root strength in areas with nonuniform tree distributions. Although our geometric root network model may capture the general characteristics of root reinforcement related to nearby trees, it cannot account for variability in the distribution and diameter of roots because of influences not addressed in our model. The tensile reinforcement correlations (Fig. 12) may be useful as a first-order approximation for relating root strength and the spatial distribution of trees across potentially unstable hillslopes. Recognizing that nearly half of the root strength of the silcrk1 site derives from two particularly large roots, our approach may benefit from more detailed root network descriptions. Additional data relating the dbh of hardwood trees to the radius of their root networks will also improve this approach. The methodology described here may also be combined with remote sensing techniques (e.g., Magnussen and Boudewyn 1998) to quantify the spatial distribution of root strength in forested terrain.

Conclusions

The variability of tree size, species, and condition (as controlled by land-use practices, fires, tree senescence, climate change, and other factors) is reflected in the subsurface character of root networks. Slope stability calculations and field observations suggest that the evolving mosaic of root strength observed in forests has a first-order impact on shallow landsliding. In contrast to previous studies, which link vegetation and slope stability by assuming that the root strength estimated for an individual tree applies across an entire landscape, we used the variance in canopy composition and distribution near landslides to quantify the effect of roots on the shear strength of soils. To explore how local vegetation may affect landslide occurrence in forested slopes in the OCR, we documented landslides following storms in 1996, quantified root strength along the lateral margins of landslide scarps, and mapped the distribution of nearby trees. The local canopy structure varied tremendously both within and amongst our study areas and likely reflects the legacy of land-use, including fire and timber harvesting. In an industrial forest that underwent widespread burning in the 19th century (Mapleton), we observed sparse conifer trees adjacent to 21 landslide scarps, whereas short-lived, shallow-rooting hardwood trees, particularly red alder and vine maple, were abundant. In a historically clearcut and commercially thinned stand with 100+ year-old trees (ESF), we observed similar numbers of live conifer and hardwood trees surrounding 11 landslide scarps, although the conifer roots displayed diseased characteristics and decreased tensile strength. We formulated a simple, geometric model for root strength using tree maps and estimates of root tensile strength for 12 landslides and 4 soil pits. Although our root strength model does not account for the complexities of root networks, it captures how their size and proximity to landslide scarps may affect the magnitude of root reinforcement. Using our proposed model, root tensile strength (and apparent cohesion because of roots) may be estimated from data describing the position, size, species, and condition of trees on soil-mantled hillslopes, thus providing a tool for hazard assessment and timber resource evaluations.

Acknowledgments

The authors thank Oregon Department of Forestry employees, particularly Jim Paul, Liz Dent, George Robison, and Keith Mills, for sharing the preliminary results of their extensive landslide inventory study, and Douglas Maguire

(Oregon State University) for providing data on the physical characteristics of Douglas-fir. The clarity and technical merit of the manuscript were improved by the comments of two anonymous reviewers and the Associate Editor. The authors appreciate their consideration and patience during the review process.

References

Abe, K., and Ziemer, R.R. 1991. Effect of tree roots on shallow-seated landslides. General Technical Report PSW-GTR 130, United States Forest Service, Washington, D.C.

Amaranthus, M.P., Rice, R.M., Barr, N.R., and Ziemer, R.R. 1985. Logging and forest roads related to increased debris slides in southwestern Oregon. Journal of Forestry, **83**: 229–233.

Bailey, J.D., Mayrsohn, C., Doescher, P.S., St. Pierre, E., and Tappeiner, J.C. 1998. Understory vegetation in old and young Douglas-fir forests of western Oregon. Forest Ecology and Management, **112**: 289–302.

Benda, L.E. 1990. The influence of debris flows on channels and valley floors in the Oregon Coast Range, U.S.A. Earth Surface Processes and Landforms, **15**: 457–466.

Benda, L., and Dunne, T. 1997. Stochastic forcing of sediment supply to channel networks from landsliding and debris flow. Water Resources Research, **33**: 2849–2863.

Bovis, M.J., and Jakob, M. 1999. The role of debris supply to determine debris flow activity in southwestern British Columbia. Earth Surface Processes and Landforms, **24**: 1039–1054.

Brown, G.W., and Krygier, J.T. 1971. Clear-cut logging and sediment production in the Oregon Coast Range. Water Resources Research, **7**: 1189–1198.

Buchanan, P., and Savigny, K.W. 1990. Factors controlling debris avalanche initiation. Canadian Geotechnical Journal, **27**: 659–675.

Burroughs, E.R., Jr. 1985. Landslide hazard rating for the Oregon Coast Range. *In* Watershed management in the eighties. *Edited by* E.B. Jones and T.J. Ward. American Society of Civil Engineers, Denver, Colo., pp. 132–139.

Burroughs, E.R., Jr., and Thomas, B.R. 1977. Declining root strength in Douglas-fir after felling as a factor in slope stability. Research Paper INT-190, United States Forest Service, Washington, D.C., 27 pp.

Coutts, M.P. 1983. Root architecture and tree stability. Plant and Soil, **71**: 171–188.

Cuthbertson, J.G. 1992. Geotechnical evaluation of the slope stability computer program 3-D LISA. Ph.D. thesis, University of Idaho, Moscow, Idaho., 272 pp.

Dietrich, W.E., and Dunne, T. 1978. Sediment budget for a small catchment in mountainous terrain. Zeitschrift für Geomorphologie, Supplement, **29**: 191–206.

Dietrich, W.E., Reiss, R., Hsu, M.-L., and Montgomery, D.R. 1995. A process-based model for colluvial soil depth and shallow landsliding using digital elevation data. Hydrological Processes, **9**: 383–400.

Eis, S. 1974. Root system morphology of Western hemlock, Western red cedar, and Douglas-fir. Canadian Journal of Forestry Research, **4**: 28–38.

Eis, S. 1987. Root systems of older immature hemlock, cedar, and Douglas-fir. Canadian Journal of Forestry, **17**: 1348–1354.

Fannin, R.J., and Rollerson, T.P. 1993. Debris flows: some physical characteristics and behaviour. Canadian Geotechnical Journal, **30**: 71–81.

Fannin, R.J., Wise, M.P., Wilkinson, J.M.T., Thomson, B., and Hetherington, E.D. 1997. Debris flow hazard assessment in British Columbia. *In* Proceedings of the 1st International Conference on Debris-flow Hazards Mitigation; Mechanics, Prediction and Assessment. *Edited by* C. Chen. American Society of Civil Engineers, Reston, Va., pp. 197–206.

Gray, D.H., and Sotir, D.B. 1996. Biotechnical and soil bioengineering slope stabilization. John Wiley & Sons, New York, 378 pp.

Iverson, R.M. 2000. Landslide triggering by rain infiltration. Water Resources Research, **36**: 1897–1910.

Iverson, R.M., and Reid, M.E. 1992. Gravity-driven groundwater flow and slope failure potential; 1, Elastic effective-stress model. Water Resources Research, **28**: 925–938.

Iverson, R.M., Reid, M.E., and LaHusen, R.G. 1997. Debris-flow mobilization from landslides. Annual Reviews of Earth and Planetary Science, **25**: 85–138.

Johnson, A.M., and Rodine, J.R. 1984. Debris flow. *In* Slope instability. *Edited by* D. Brunsden and D.B. Prior. Wiley & Sons, London, pp. 257–361.

Johnson, K.A., and Sitar, N. 1990. Hydrologic conditions leading to debris-flow initiation. Canadian Geotechnical Journal, **27**: 789–801.

Ketcheson, G.L., and Froehlich, H.A. 1978. Hydrology factors and environmental impacts of mass soil movements in the Oregon Coast Range. Water Resources Research Institute, Oregon State University, Corvallis, Oreg., 94 pp.

Kochenderfer, J.N. 1973. Root distribution under forest types native to West Virginia. Ecology, **54**: 445–448.

Krogstad, F. 1995. A physiology and ecology based model of lateral root reinforcement of unstable hillslopes. M.Sc. thesis, University of Washington, Seattle, Wash.

Kuruppuarachchi, T., and Wyrwoll, K.-H. 1992. The role of vegetation clearing in the mass failure of hillslopes: Moresby Ranges, Western Australia. Catena, **19**: 193–208.

Lambe, T.W., and Whitman, R.V. 1969. Soil mechanics. John Wiley & Sons, New York, 553 pp.

Magnussen, S., and Boudewyn, P. 1998. Derivations of stand heights from airborne laser scanner data with canopy-based quantile estimators. Canadian Journal of Forest Research, **28**: 1016–1031.

Maguire, D.A., and Hann, D.W. 1989. The relationship between gross crown dimensions and sapwood area at crown base in Douglas-fir. Canadian Journal of Forest Research, **19**: 557–565.

May, C.L. 1998. Debris flow characteristics associated with forest practices in the Central Oregon Coast Range. M.S. thesis, Oregon State University, Corvallis, Oreg., 121 pp.

McMinn, R.G. 1963. Characteristics of Douglas-fir root systems. Canadian Journal of Botany, **41**: 105–122.

Montgomery, D.R., and Dietrich, W.E. 1994. A physically based model for the topographic control on shallow landsliding. Water Resources Research, **30**: 1153–1171.

Montgomery, D.R., Dietrich, W.E., Torres, R., Anderson, S.P., Heffner, J.T., and Loague, K. 1997. Hydrologic response of a steep, unchanneled valley to natural and applied rainfall. Water Resources Research, **33**: 91–109.

Montgomery, D.R., Schmidt, K.M., Dietrich, W.E., and Greenberg, H. 2000. Forest clearing and regional landsliding. Geology, **28**: 311–314.

Okimura, T. 1983. A slope stability method for predicting rapid mass movements on granite mountain slope. Journal of Natural Disaster Science, **5**: 13–30.

Okunishi, K., and Iida, T. 1981. Evolution of hillslopes including landslides. Transactions, Japanese Geomorphological Union, **2**: 291–300.

O'Loughlin, C.L. 1974. The effect of timber removal on the stability of forest soils. Journal of Hydrology, **13**: 121–134.

Pierson, T.C. 1977. Factors controlling debris-flow initiation on forested hillslopes in the Oregon Coast Range. Ph.D. thesis, University of Washington, Seattle, Wash., 166 pp.

Reid, M.E., and Iverson, R.M. 1992. Gravity-driven groundwater flow and slope failure potential; 2, Effects of slope morphology, material properties, and hydraulic heterogeneity. Water Resources Research, **28**: 939–950.

Reneau, S.L. 1988. Depositional and erosional history of hollows; application to landslide location and frequency, long-term erosion rates, and the effects of climatic change. Ph.D. thesis, University of California, Berkeley, Calif., 327 pp.

Reneau, S.L., and Dietrich, W.E. 1987. Size and location of colluvial landslides in a steep forested landscape. *In* International Symposium on Erosion and Sedimentation in the Pacific Rim, Corvallis, Oreg., *Edited by* R.L. Beschta, T. Blinn, G.E. Grant, G.G. Ice, and F.J. Swanson. International Association of Hydrological Sciences (IAHS) Publication No. 165, IAHS Press, Wallingford, Oxon, U.K., pp. 39–48.

Reneau, S.L., and Dietrich, W.E. 1990. Depositional history of hollows on steep hillslopes, coastal Oregon and Washington. National Geographic Research, **6**: 220–230.

Riestenberg, M.M. 1994. Anchoring of thin colluvium by roots of sugar maple and white ash on hillslopes in Cincinnati. United States Geological Survey Bulletin, **2059-E**: 1–25.

Riestenberg, M.M., and Sovonick-Dunford, S. 1983. The role of woody vegetation in stabilizing slopes in the Cincinnati area, Ohio. Geological Society of America Bulletin, **15**: 3–45.

Robison, E.G., Mills, K., Paul, J., Dent, L., and Skaugset, A. 1999. Storm impacts and landslides of 1996: Final report. Forest Practices Technical Report Number 4, Oregon Department of Forestry, Salem, 145 pp.

Rollerson, T.P., Thomson, B., and Millard, T.H. 1997. Identification of coastal British Columbia terrain susceptible to debris flows. *In* Proceedings of the 1st International Conference on Debris-flow Hazards Mitigation; Mechanics, Prediction and Assessment. *Edited by* C. Chen. American Society of Civil Engineers, Reston, Va., pp. 484–495.

Ross, C.R. 1932. Root development of western conifers. M.Sc. thesis, University of Washington, Seattle, Wash., 63 pp.

Schmidt, K.M. 1999. Root strength, colluvial soil depth, and colluvial transport on landslide-prone hillslopes. Ph.D. thesis, University of Washington, Seattle, Wash., 258 pp.

Schmidt, K.M., Roering, J.J., Stock, J.D., Dietrich, W.E., Montgomery, D.R., and Schaub, T. 2001. Root cohesion variability and shallow landslide susceptibility in the Oregon Coast Range. Canadian Geotechnical Journal, **38**: 995–1024.

Schroeder, W.L., and Alto, J.V. 1983. Soil properties for slope stability analysis; Oregon and Washington Coastal mountains. Forest Science, **29**: 823–833.

Shainsky, L.J., Newton, M., and Radosevich, S.R. 1992. Effects of intra-specific and inter-specific competition on root and shoot biomass of young Douglas-fir and red alder. Canadian Journal of Forest Research, **22**: 101–110.

Shewbridge, S.E., and Sitar, N. 1989. Deformation characteristics of reinforced sand in direct shear. Journal of Geotechnical Engineering, **115**: 1134–1147.

Sidle, R.C. 1992. A theoretical model of the effects of timber harvesting on slope stability. Water Resources Research, **28**: 1897–1910.

Sidle, R.C., and Wu, W.M. 1999. Simulating effects of timber harvesting on the temporal and spatial distribution of shallow landslides. Zeitschrift für Geomorphologie, **43**: 185–201.

Skaugset, A. 1997. Modeling root reinforcement in shallow forest soils. Ph.D. thesis, Oregon State University, Corvallis, Oreg., 456 pp.

Smith, J.H.G. 1964. Root spread can be estimated from crown width of Douglas fir, lodgepole pine, and other British Columbia tree species. Forest Chronicle, **40**: 456–473.

Snyder, K. 2000. Debris flows and flood disturbance in small mountain watersheds. M.S. thesis, Oregon State University, Corvallis, Oreg., 52 pp.

Spies, T.A., and Franklin, J.F. 1991. The structure of natural young, mature, and old-growth Douglas-fir forests in Oregon and Washington [U.S.A.]. General Technical Report PNW 285, United States Forest Service, Washington, D.C., pp. 91–110.

Stolzy, L.H., and Barley, K.P. 1968. Mechanical resistance encountered by roots entering compact soils. Soil Science, **105**: 297–301.

Stone, E.L., and Kalisz, P.J. 1991. On the maximum extent of tree roots. Forest Ecology and Management, **46**: 59–102.

Swanson, F.J., Swanson, M.M., and Woods, C. 1981. Analysis of debris-avalanche erosion in steep forest lands: An example from Mapleton, Oregon, U.S.A. *In* Erosion and sediment transport in the Pacific Rim Steeplands. *Edited by* T.R.H. Davies and A.J. Pearce. International Association of Hydrological Sciences Publication No. 132, IAHS Press, Wallingford, Oxon, U.K., pp. 67–75.

Swanston, D.N., and Swanson, F.J. 1976. Timber harvesting, mass erosion, and steepland forest geomorphology in the Pacific Northwest. *In* Geomorphology and engineering. *Edited by* D.R. Coates. Van Nostrand Reinhold, New York, pp. 199–221.

Swanston, D.N., Lienkaemper, G.W., Mersereau, R.C., and Levno, A.B. 1988. Timber harvest and progressive deformation of slopes in southwestern Oregon. Bulletin of the Association of Engineering Geologists, **25**: 371–381.

Taylor, G. 1997. Causes of the flood and a comparison to other climate events. *In* The Pacific Northwest Floods of February 6–11, 1996: Proceedings of the Pacific Northwest Water Issues Conference. *Edited by* A. Laenen, American Institute of Hydrology, Portland, Oreg., pp. 3–7.

Terwilliger, V.J., and Waldron, L.J. 1991. Effects of root reinforcement on soil-slip patterns in the Transverse Ranges of southern California. Geological Society of America Bulletin, **103**: 775–785.

Trappe, J.M., Franklin, J.F., Tarrant, R.F., and Hansen, G.M. 1968. Biology of alder, 40th Northwest Scientific Association Meeting, Pacific Northwest Forest and Range Experiment Station. USDA Forest Service, Portland, Oreg., 292 pp.

United States Geological Survey. 1898. Map showing location and extent of the forest reserves and national parks in western United States. Julius Bien & Co., New York.

Van Pelt, R., and Franklin, J.F. 1999. Response of understory trees to experimental gaps in old-growth Douglas-fir forests. Ecological Applications, **9**: 504–512.

Waldron, L.J. 1977. The shear resistance of root-permeated homogeneous and stratified soil. Soil Science Society of America Journal, **41**: 843–849.

Waldron, L.J., and Dakessian, S. 1981. Soil reinforcement by roots: calculation of increased soil shear resistance from root properties. Soil Science, **132**: 427–435.

Wardman, C.W., and Schmidt, M.G. 1998. Growth and form of Douglas-fir adjacent to persistent vine maple gaps in southwestern British Columbia. Forest Ecology and Management, **106**: 223–233.

Watson, A., Phillips, C., and Marden, M. 1999. Root strength, growth, and rates of decay: root reinforcement changes of two

tree species and their contribution to slope stability. Plant and Soil, **217**: 39–47.

Wilson, C.J., and Dietrich, W.E. 1987. The contribution of bedrock groundwater flow to storm runoff and high pore pressure development in hollows. *In* Erosion and sedimentation in the Pacific Rim. *Edited by* R.L. Beschta, T. Blinn, G.E. Grant, G.G. Ice, and F.J. Swanson. International Association of Hydrological Sciences (IAHS) Publication 165, IAHS Press, Wallingford, Oxon, U.K., pp. 49–59.

Worthington, N.P., Ruth, R.H., and Matson, E.E. 1962. Red alder: its management and utilization. Miscellaneous Publication 881, U.S. Department of Agriculture, Washington, D.C., 44 pp.

Wu, T.H. 1984. Effect of vegetation on slope stability. *In* Soil reinforcement and moisture effects on slope stability. Transportation Research Board, Washington, D.C., pp. 37–46.

Wu, T.H. 1995. Slope stabilization. *In* Slope stabilization and erosion control: A bioengineering approach. *Edited by* R.P.C. Morgan and R.J. Rickson. E & FN Spon, London, pp. 221–264.

Wu, W., and Sidle, R.C. 1995. A distributed slope stability model for steep forested basins. Water Resources Research, **31**: 2097–2110.

Wu, T.H., McKinnell, W.P., III, and Swanston, D.N. 1979. Strength of tree roots and landslides on Prince of Wales Island, Alaska. Canadian Geotechnical Journal, **16**: 19–33.

Yee, C.S., and Harr, D.R. 1977. Influence of soil aggregation on slope stability in the Oregon Coast Range. Environmental Geology, **1**: 367–377.

Ziemer, R.R. 1981. Roots and the stability of forested slopes. *In* Erosion and sediment transport in Pacific Rim Steeplands. *Edited by* T.R.H. Davies and A.J. Pearce. International Association of Hydrological Sciences Publication No. 132, IAHS Press, Wallingford, Oxon, U.K., pp. 343–361.